

The reaction $^2H(\gamma, \pi^0)np$ in the threshold region

M.I. Levchuk^a ^{*}, M. Schumacher^b [†] and F. Wissmann^b [‡]

^a*B.I. Stepanov Institute of Physics, Belarus National Academy of Sciences,
F. Scaryna prospect 70, Minsk 220072, Belarus*

^b*II Physikalisches Institut der Universität Göttingen,
Bunsenstraße 7-9, D-37073 Göttingen, Germany*

Abstract

Neutral pion photoproduction on the deuteron in the inelastic channel is studied in the threshold region from 142 to 160 MeV. The calculation is based on the use of the diagrammatic approach. Contributions from the pole diagrams, one-loop diagrams both with $n-p$ and $\pi-N$ rescattering as well as two-loop diagrams with simultaneous inclusion of these rescattering mechanisms are taken into account. We have found a reasonable agreement with a very simple calculation by J.C. Bergstrom et al. [Phys. Rev. C 57 (1998) 3203]. It is shown that the ‘effective’ electric dipole deuteron amplitude E_d is negative in agreement with a prediction of ChPT. We conclude that a deviation of about 20% from a ChPT prediction for E_d discovered in an experiment on coherent π^0 photoproduction off the deuteron cannot be attributed to inadequate estimates of inelastic channel contributions. We suggest that $\pi-N$ rescattering is responsible for the deviation of the free-nucleon p_1 threshold amplitude from the value measured in that experiment.

PACS: 25.20.Lj; 25.45.De

Keywords: Pion photoproduction; Low-energy parameters; Deuteron

I. INTRODUCTION

Nowadays, the threshold s - and p - amplitudes of π^0 photoproduction off the deuteron are of considerable theoretical and experimental interest. This is motivated by two reasons.

^{*}E-mail: levchuk@dragon.bas-net.by

[†]E-mail: schumacher@physik2.uni-goettingen.de

[‡]E-mail: fwissma@gwdg.de

Firstly, the deuteron is a natural ‘source’ of neutrons. If one wants to minimize uncertainties stemming from nuclear forces when extracting neutron threshold parameters one should use a deuteron target. At present, there is a significant disagreement for values of the threshold electric dipole amplitude $E_{0+}^{n\pi^0}$ calculated in chiral perturbation theory (ChPT) and dispersion theory (DR), respectively, 2.13 [1] and 1.19 [2] (in units of $10^{-3}/\mu_{\pi^+}$ which are suppressed from here on). At the same time the predicted values for $E_{0+}^{p\pi^0}$ agree reasonably with each other (−1.16 and −1.22, respectively) and with experimental values -1.32 ± 0.08 [3] and -1.31 ± 0.08 [4]. Resolving the problem mentioned in favour of the one or the other theory requires experimental measurements of which in the reactions $\gamma d \rightarrow \pi^0 d$ and $ed \rightarrow e' \pi^0 d$ seem to be most promising. However, even in these simplest reactions many theoretical problems in the extraction of neutron data are anticipated.

On the other hand, the deuteron cannot be considered as a direct sum of the proton and neutron (impulse approximation). Photons may also interact with potential (virtual) mesons. This effect is known as ‘Meson Exchange Currents’ (MEC). It was found to be very important in the case of coherent neutral pion photoproduction on the deuteron [5]. Accepting the ChPT predictions for free nucleons we could expect in the impulse approximation a value of about $+0.5$ ($= \frac{1}{2}[E_{0+}^{p\pi^0} + E_{0+}^{n\pi^0}]$) for the deuteron electric dipole amplitude E_d . In fact, however, the ChPT result is quite different being about -1.8 ± 0.2 [5] and the difference is due to the meson exchange contributions.

A very recent measurement of E_d performed at SAL [6] in coherent π^0 photoproduction on the deuteron within 20 MeV of threshold has given a value of -1.45 ± 0.09 which is about 20% lower than the ChPT prediction. There is also a significant deviation from the ChPT prediction for the free-nucleon p_1 amplitude. A comparison of the differential cross sections calculated in a theoretical model [7] with the data revealed a noticeable disagreement as well. It was claimed in Ref. [7] that a possible reason for the disagreements might consist in inadequate treatment of the inelastic channel in Ref. [6]. Since the $^2H(\gamma, \pi^0)np$ reaction cannot be resolved one has to estimate its contribution to the coherent channel making the use of theoretical predictions. Indeed, a model developed in Ref. [6] seems to be oversimplified. For example, the authors employed a square-well deuteron wave function and used the effective range approximation to describe the final state $n-p$ interaction. The deuteron d -wave was ignored. Explicit calculations of very important diagrams with $\pi-N$ rescattering were not carried out. Effectively these latter were included into the model by accepting the extracted value -1.45 for E_d which, as it has been noted, contains contributions from MEC or, in other words, from $\pi-N$ rescattering. Although a theoretical uncertainty of $\pm 25\%$, based on input parameters, was assigned in Ref. [6] to the calculated cross sections it would be desirable to have more realistic calculations for the inelastic channel.

The present paper is aimed at fixing the defects of the model [6]. We are going to study whether these defects may be responsible for the deviations mentioned. In our previous paper [8] on the reaction

$$\gamma d \rightarrow \pi^0 np \quad (1.1)$$

we restricted ourselves to the energy region 200 to 400 MeV. Now we extend the model to the threshold region. The extension includes: i) a more realistic treatment of the π^0 photoproduction amplitudes at threshold energies; ii) in Ref. [8] we considered $\pi-N$ rescattering mechanism but without taking into account the $n-p$ rescattering process which may

follow π - N rescattering. In the present paper a corresponding diagram has been taken into account. We would like to emphasize that the study of the process (1.1) in the threshold region is hardly of theoretical interest in its own. Rather it is needed for experimentalists to estimate the relative contribution of the inelastic channel to the cross section of coherent pion photoproduction on the deuteron. Furthermore, these studies may be useful for extracting the elementary $E_{0+}^{n\pi^0}$ amplitude from exclusive inelastic data where the recoil neutron is detected.

II. KINEMATICS

Let us denote by $k = (\omega, \mathbf{k})$, $p_d = (\varepsilon_d, -\mathbf{k})$, $q = (\varepsilon_\pi, \mathbf{q})$, $p_n = (\varepsilon_n, \mathbf{p}_n)$ and $p_p = (\varepsilon_p, \mathbf{p}_p)$ the 4-momenta of the initial photon and deuteron and the final pion, neutron and proton, respectively in the γ - d c.m. frame. A symbol E_γ we reserve for the lab photon energy $E_\gamma = W_{\gamma d}\omega/m_d$ with $W_{\gamma d} = \omega + \varepsilon_d = \omega + \sqrt{\omega^2 + m_d^2}$ and m_d being the deuteron mass. It is convenient to take as independent kinematical variables the photon energy and pion angle, Θ_π , in the c.m. frame and momentum \mathbf{p} of one of the nucleons - say, the neutron - in the final n - p c.m. frame (see Ref. [6]). Once these variables have been specified the pion momentum can be easily found:

$$|\mathbf{q}| = \frac{1}{2W_{\gamma d}} \sqrt{[W_{\gamma d}^2 - (W_{np} + \mu)^2][W_{\gamma d}^2 - (W_{np} - \mu)^2]}, \quad (2.1)$$

where $W_{np} = 2\sqrt{\mathbf{p}^2 + m^2}$ (m is the nucleon mass) and μ is the π^0 mass. Then making a boost with the velocity $-\mathbf{q}/(W_{\gamma d} - \varepsilon_\pi)$ we obtain the neutron momentum p_n and, therefore, totally restore the kinematics in the γ - d c.m. frame. Note that in kinematic calculations a distinction is not made between the proton and neutron masses. It is, however, taken into account in the threshold π^0 photoproduction amplitude when parametrizing the s - and p -waves multipoles (see Sect. III, Eq. (3.2)).

The differential cross section is

$$\frac{d^4\sigma}{d\mathbf{p}d\Omega_\pi} = \frac{1}{(2\pi)^5} \frac{2m^2\varepsilon_d|\mathbf{q}|^3}{4\omega W_{\gamma d}W_{np}(\varepsilon_\pi q \cdot p_p - \varepsilon_p \mu^2)} \frac{1}{6} \sum_{m_p m_n \lambda m_d} |\langle m_p m_n | T | \lambda m_d \rangle|^2, \quad (2.2)$$

where m_p , m_n , λ , and m_d are spin states of the proton, neutron, photon, and deuteron, respectively.

Assuming that near threshold energies the nucleons are not detected we should integrate the l.h.s. of Eq. (2.2) over the momentum \mathbf{p} to obtain

$$\frac{d\sigma}{d\Omega_\pi} = \int_0^{p^{max}} \frac{d^4\sigma}{d\mathbf{p}d\Omega_\pi} p^2 dp d\Omega_\mathbf{p}, \quad (2.3)$$

where the maximum value p^{max} is found from energy-momentum conservation and reads

$$p^{max} = \frac{1}{2} \sqrt{(W_{\gamma d} - \mu)^2 - 4m^2}. \quad (2.4)$$

III. THEORETICAL MODEL FOR THE $\gamma D \rightarrow \pi^0 NP$ PROCESS

The scattering amplitude of the reaction (1.1) is described as a sum of contributions from diagrams which are expected to be most important in the energy region under consideration. The pole diagrams *a* and *b* in Fig. 1 and one-loop diagram 1*c* correspond to the impulse approximation without and with *n-p* interaction in the final state, respectively. The necessity to consider the latter mechanism follows from the very strong nucleon-nucleon interaction at small energies. It might seem that diagrams 1*d* to *f* with π -*N* rescattering could be disregarded in the threshold region since the π -*N* scattering lengths are about two orders smaller than those for *n-p* scattering. In fact, however, there is actually no suppression of the diagrams 1*d* to *f* in comparison with diagram 1*c*. Indeed, keeping in mind that the threshold electric dipole amplitudes E_{0+} for charged channels are about 30 times larger in absolute numbers than those for the neutral channels one can expect the corresponding contributions from π -*N* rescattering to be of the same order as the ones from final state *n-p* interaction. This expectation will be confirmed below by numerical calculations. A very big effect of π -*N* rescattering in the case of coherent π^0 photoproduction on the deuteron in the threshold region was also found in Refs. [9,10,7]. Note that our treatment of π -*N* contribution is similar to the one of ‘three-body interactions to order q^3 ’ from Ref. [5] in the case of coherent π^0 photoproduction off the deuteron. It was found in that paper that three-body contributions at order q^4 are less important. Based on this finding we do not take into account the corresponding diagrams for the reaction (1.1) though they of course exist.

We begin with the pole diagrams. The matrix element corresponding to the diagram in Fig. 1*a* reads

$$\langle m_p m_n | T^{1a}(\mathbf{k}, \mathbf{q}, \mathbf{p}_p) | \lambda m_d \rangle = \sum_{m_{\tilde{n}}} \Psi_{m_p m_{\tilde{n}}}^{m_d} \left(\mathbf{p}_p + \frac{\mathbf{k}}{2} \right) \langle m_n | T_{\gamma \tilde{n} \rightarrow \pi^0 n}(\mathbf{k}_{\pi n}, \mathbf{q}_{\pi n}) | \lambda m_{\tilde{n}} \rangle, \quad (3.1)$$

where $\Psi_{m_p m_{\tilde{n}}}^{m_d}(\mathbf{p}_p + \mathbf{k}/2)$ is the deuteron wave function (DWF) and $\langle m_n | T_{\gamma n \rightarrow \pi^0 n} | \lambda m_{\tilde{n}} \rangle$ is the amplitude of the elementary process $\gamma n \rightarrow \pi^0 n$. The amplitude depends on photon ($\mathbf{k}_{\pi n}$) and pion ($\mathbf{q}_{\pi n}$) momenta taken in the c.m. frame of the π -*n* pair. These momenta can be obtained from the corresponding momenta in the γ -*d* c.m. frame through a boost with the velocity $\mathbf{p}_p/(W_{\gamma d} - \varepsilon_p)$.

In calculations we used DWF for non-relativistic versions of the Bonn OBE potential [11,12] (the same models were used when solving the Lippmann-Schwinger equation for the *n-p* scattering amplitude needed for calculations of diagrams 1*c* and *f*, see below). Analytical parametrizations of the *s*- and *d*-wave amplitudes were taken from Ref. [13]. We would like to note just here that our results are practically independent of the choice of the potentials.

In our previous paper [8] we used the well-known Blomqvist-Laget parametrization [14] of the pion photoproduction amplitudes. This model is rather simple and, nevertheless, fits reasonably to the experimental data. Unfortunately, it is obsolete in the sense that it predicts the threshold electric dipole amplitudes for the neutral channels in accordance with the classical low-energy theorem, $E_{0+}^{p\pi^0} = -2.4$ and $E_{0+}^{n\pi^0} = 0.4$, but in disagreement with the modern values (see Sect. I). To be consistent with these latter, we use in the energy region $\omega \leq 150$ MeV a parametrization for the neutral pion photoproduction amplitude given in

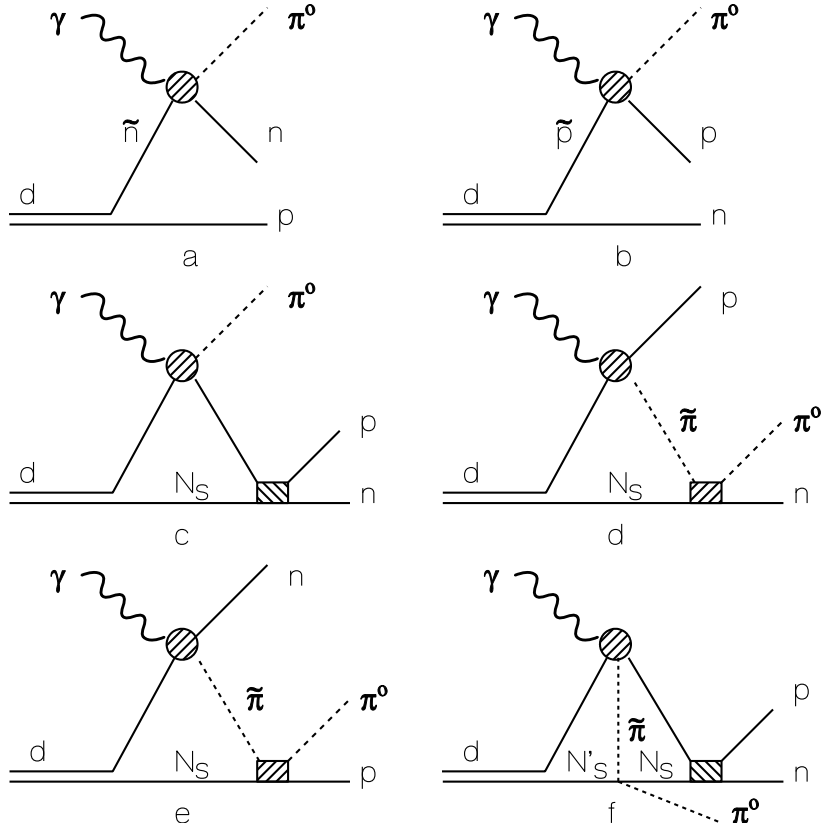


FIG. 1. Diagrammatic representation of the scattering amplitude.

Ref. [7]. The threshold amplitude in the γ - N c.m. frame can be written in the following form [1]

$$T_{\gamma N \rightarrow \pi^0 N} = -\frac{4\pi W_{\gamma N}}{m} [i\boldsymbol{\sigma} \cdot \boldsymbol{\epsilon} (E_{0+} + \mathbf{k} \cdot \mathbf{q} p_1) + i\boldsymbol{\sigma} \cdot \mathbf{k} \boldsymbol{\epsilon} \cdot \mathbf{q} p_2 + \mathbf{q} \cdot (\mathbf{k} \times \boldsymbol{\epsilon}) p_3], \quad (3.2)$$

where $W_{\gamma N}$ is the total energy of the γ - N system, and p_1 , p_2 and p_3 are the p -waves multipoles. The E_{0+} amplitude was taken in the form of Eq. (25) of Ref. [7] with parameters from Table I of the same work. The parametrization takes into account the energy dependence of the E_{0+} multipole as well as the so-called cusp effect. Just at threshold it reproduces the ChPT and DR values (see Sect. I). These parametrizations were used in the present paper to study uncertainties due to the choice of a theoretical model for pion photoproduction. As to the p -wave amplitudes, they are also taken for two models and listed in Table I. As was shown in Ref. [7], the parametrizations corresponding to ChPT and DR reproduce very well the available data on the energy dependence of the real part of E_{0+} as well as the total and differential cross sections of the reaction $\gamma p \rightarrow \pi^0 p$ up to $E_\gamma \simeq 180$ MeV.

One should emphasize that, although we are going to work in the energy region below 160 MeV, we need parametrizations for the photoproduction amplitudes at higher energies

TABLE I. Threshold p -waves amplitudes (units are $10^{-3}/\mu_{\pi^+}^3$).

	p_1		p_2		p_3	
	$\pi^0 p$	$\pi^0 n$	$\pi^0 p$	$\pi^0 n$	$\pi^0 p$	$\pi^0 n$
ChPT	10.3	7.4	-11.0	-8.4	11.7	11.1 ^a
DR	10.5	7.8	-11.4	-8.8	10.2	9.5 ^a

^aThe value was obtained from isospin relations between four physical channels.

too. Such energies emerge because of two kinds of boosts. The first one occurs at the integration over \mathbf{p} in Eq. (2.3). Below 160 MeV the value of p^{max} does not exceed 125 MeV/c so that the corresponding boosts lead to only small energy shifts. But at integrations over loops when calculating n - p final state interaction and π - N rescattering (see below), energy shifts can be much bigger. In addition, when considering π - N rescattering the pion photoproduction amplitudes for the charged channels are also needed. Both these latter and the π^0 photoproduction amplitudes at photon c.m. energies above 150 MeV were taken from the Blomqvist-Laget model [14].

In full analogy with Eq. (3.1) we write the matrix element corresponding to diagram 1*b* in the form

$$\langle m_p m_n | T^{1b}(\mathbf{k}, \mathbf{q}, \mathbf{p}_n) | \lambda m_d \rangle = \sum_{m_{\tilde{p}}} \Psi_{m_n m_{\tilde{p}}}^{m_d} \left(\mathbf{p}_n + \frac{\mathbf{k}}{2} \right) \langle m_p | T_{\gamma \tilde{p} \rightarrow \pi^0 p}(\mathbf{k}_{\pi p}, \mathbf{q}_{\pi p}) | \lambda m_{\tilde{p}} \rangle. \quad (3.3)$$

The photon ($\mathbf{k}_{\pi p}$) and pion ($\mathbf{q}_{\pi p}$) momenta in the c.m. frame of the π - p pair can be obtained by boosting the corresponding momenta in the γ - d c.m. frame with the velocity $\mathbf{p}_n/(W_{\gamma d} - \varepsilon_n)$.

The one-loop diagram in Fig. 1*c* with n - p rescattering in the final state is expected to be very important in the energy region under consideration. The smallness of the relative n - p momenta leads to strong 1S_0 - and 3S_1 -wave interactions which significantly modify the n - p plane wave states appearing in the pole diagrams 1*a* and *b*. The matrix element corresponding to diagram 1*c* is

$$\begin{aligned} \langle m_p m_n | T^{1c}(\mathbf{k}, \mathbf{q}, \mathbf{p}_n) | \lambda m_d \rangle = & -m \int \frac{d^3 \mathbf{p}_s}{(2\pi)^3} \frac{1}{p_{in}^2 - p_{out}^2 - i0} \\ & \times \sum_{m_{\tilde{p}} m_{\tilde{n}}} \left[\langle \mathbf{p}_{out}, m_p m_n | T_{np} | -\mathbf{p}_{in}, m_{\tilde{p}} m_{\tilde{n}} \rangle \langle m_{\tilde{p}} m_{\tilde{n}} | T^{1a}(\mathbf{k}, \mathbf{q}, \mathbf{p}_s) | \lambda m_d \rangle \right. \\ & \left. + \langle \mathbf{p}_{out}, m_p m_n | T_{np} | \mathbf{p}_{in}, m_{\tilde{p}} m_{\tilde{n}} \rangle \langle m_{\tilde{p}} m_{\tilde{n}} | T^{1b}(\mathbf{k}, \mathbf{q}, \mathbf{p}_s) | \lambda m_d \rangle \right], \end{aligned} \quad (3.4)$$

where $\mathbf{p}_{out} = (\mathbf{p}_p - \mathbf{p}_n)/2$ and $\mathbf{p}_{in} = \mathbf{p}_s + \mathbf{q}/2$ are the relative momenta of the n - p pair after and before scattering, respectively, and $\langle \mathbf{p}_{out}, m_p m_n | T_{np} | \mathbf{p}_{in}, m_{\tilde{p}} m_{\tilde{n}} \rangle$ being the half off-shell n - p scattering amplitude. We will not discuss here details of computations of the amplitude (3.4) because they are given in Ref. [8]. Note only that all partial waves with the total angular momentum $J \leq 1$ were retained in the n - p scattering amplitude. We cut off the integration in Eq. (3.4) at $|\mathbf{p}_s|^{max} = 500$ MeV/c since it is difficult to control the pion photoproduction amplitudes at higher momenta. Such a cutting off has no impact on our

final results because the integral is mainly saturated at smaller momenta. For example, a variation of $|\mathbf{p}_s|^{max}$ from 400 to 500 MeV changes the calculated differential cross sections by less than 2%. One further remark is concerned with the choice of particle energies when integrating over the momenta \mathbf{p}_s . In accordance with a prescription of Ref. [15] we will suppose a spectator particle (it is denoted in Fig. 1c by a subscript s) to be on its mass shell.

The amplitude for the diagram in Fig. 1d reads

$$\begin{aligned} \langle m_p m_n | T^{1d}(\mathbf{k}, \mathbf{q}, \mathbf{p}_n) | \lambda m_d \rangle = & - \int \frac{d^3 \mathbf{p}_s^*}{(2\pi)^3} \sum_{m_1 m_2} \Psi_{m_1 m_2}^{m_d} \left(\mathbf{p}_s + \frac{\mathbf{k}}{2} \right) \left\{ \frac{\varepsilon_n^* + \varepsilon_s^*}{2W_{\pi n}} \frac{1}{p_s^{*2} - p_{\pi n}^{*2} - i0} \right. \\ & \times \left[\langle m_n | T_{\tilde{\pi}^0 n \rightarrow \pi^0 n}(\mathbf{p}_{\pi n}^*, \mathbf{p}_s^*) | m_1 \rangle \langle m_p | T_{\gamma p \rightarrow \tilde{\pi}^0 p}(\mathbf{k}_{\tilde{\pi} p}, \mathbf{q}_{\tilde{\pi} p}) | m_2 \rangle \right. \\ & \left. \left. - \langle m_n | T_{\tilde{\pi}^- p \rightarrow \pi^0 n}(\mathbf{p}_{\pi n}^*, \mathbf{p}_s^*) | m_1 \rangle \langle m_p | T_{\gamma n \rightarrow \tilde{\pi}^- p}(\mathbf{k}_{\tilde{\pi} p}, \mathbf{q}_{\tilde{\pi} p}) | m_2 \rangle \right] \right\}. \end{aligned} \quad (3.5)$$

In Eq. (3.5) the asterisk denotes kinematical variables in the π^0 - n c.m. frame. $W_{\pi n} = \varepsilon_\pi^* + \varepsilon_n^* = \sqrt{p_{\pi n}^{*2} + \mu^2} + \sqrt{p_{\pi n}^{*2} + m^2}$ is the total energy in this frame and

$$p_{\pi n}^{*2} = \frac{1}{4W_{\pi n}^2} [W_{\pi n}^2 - (m + \mu)^2][W_{\pi n}^2 - (m - \mu)^2] > 0. \quad (3.6)$$

A boost with the velocity $-\mathbf{p}_p/(W_{\gamma d} - \varepsilon_p)$ is needed to transform the momentum \mathbf{p}_s^* to \mathbf{p}_s in the γ - d c.m. frame. As in the case of Eq. (3.4) we cut off the integration in Eq. (3.5) at $|\mathbf{p}_s^*|^{max} = 500$ MeV/c without any noticeable changes in the calculated differential cross sections. Spectator particles in diagrams 1d and e are again supposed to be on their mass shells.

The π - N scattering amplitude has the following form

$$\begin{aligned} \langle m' | T_{\pi N \rightarrow \pi' N'}^I(\mathbf{q}', \mathbf{q}) | m \rangle = & (2\pi)^3 \sqrt{\frac{4\varepsilon_\pi^* \varepsilon_\pi'^* \varepsilon_N^* \varepsilon_N'^*}{m^2}} \\ & \times \sum_{J L m_J} C_{\frac{1}{2} m' L m'_L}^{J m_J} Y_L^{m'_L}(\hat{\mathbf{q}}') C_{\frac{1}{2} m L m_L}^{J m_J} Y_L^{m_L*}(\hat{\mathbf{q}}) T_{IJ}^L(q', q), \end{aligned} \quad (3.7)$$

where \mathbf{q}' and \mathbf{q} are the final and initial momenta of (generally, off-shell) particles in the π - N c.m. frame, $Y_L^{m_L}(\hat{\mathbf{q}})$ are the spherical harmonics, $C_{J_1 M_1 J_2 M_2}^{J M}$ are the Clebsch-Gordan coefficients. Partial wave amplitudes $T_{IJ}^L(q', q)$ for all s - and p -waves channels were obtained by solving the Lippmann-Schwinger equation for a separable energy-dependent π - N potential built in Ref. [16]. Only for the p_{33} -wave we preferred using a model from Ref. [14] with explicit inclusion of a s -channel pole diagram with an intermediate Δ isobar. Contributions from the d -waves were found to be negligible. Two π - N scattering amplitudes in isospin space are numbered by a symbol $I = \frac{1}{2}$ or $\frac{3}{2}$. Needed in Eq. (3.5) physical amplitudes are linear combinations of these isospin amplitudes:

$$\begin{aligned} T_{\pi^0 p \rightarrow \pi^0 p} &= T_{\pi^0 n \rightarrow \pi^0 n} = \frac{1}{3} \left(T^{\frac{1}{2}} + 2T^{\frac{3}{2}} \right), \\ T_{\pi^+ n \rightarrow \pi^0 p} &= -T_{\pi^- p \rightarrow \pi^0 n} = \frac{\sqrt{2}}{3} \left(T^{\frac{1}{2}} - T^{\frac{3}{2}} \right). \end{aligned} \quad (3.8)$$

In full analogy with Eq. (3.5) one has for diagram 1e

$$\begin{aligned}
\langle m_p m_n | T^{1e}(\mathbf{k}, \mathbf{q}, \mathbf{p}_p) | \lambda m_d \rangle = & \\
& - \int \frac{d^3 \mathbf{p}_s^*}{(2\pi)^3} \sum_{m_1 m_2} \Psi_{m_1 m_2}^{m_d} \left(\mathbf{p}_s + \frac{\mathbf{k}}{2} \right) \left\{ \frac{\varepsilon_p^* + \varepsilon_s^*}{2W_{\pi p}} \frac{1}{p_s^{*2} - p_{\pi p}^{*2} - i0} \right. \\
& \times \left[\langle m_p | T_{\tilde{\pi}^0 p \rightarrow \pi^0 p}(\mathbf{p}_{\pi p}^*, \mathbf{p}_s^*) | m_1 \rangle \langle m_n | T_{\gamma n \rightarrow \tilde{\pi}^0 n}(\mathbf{k}_{\tilde{\pi} n}, \mathbf{q}_{\tilde{\pi} n}) | m_2 \rangle \right. \\
& \left. \left. - \langle m_p | T_{\tilde{\pi}^+ n \rightarrow \pi^0 p}(\mathbf{p}_{\pi p}^*, \mathbf{p}_s^*) | m_1 \rangle \langle m_n | T_{\gamma p \rightarrow \tilde{\pi}^+ n}(\mathbf{k}_{\tilde{\pi} n}, \mathbf{q}_{\tilde{\pi} n}) | m_2 \rangle \right] \right\}, \quad (3.9)
\end{aligned}$$

where the meaning of all variables is easily understood from the corresponding ones in Eq. (3.5).

Finally, let us consider diagram 1f which includes simultaneously both π - N and n - p rescattering. One has for the corresponding matrix element

$$\begin{aligned}
\langle m_p m_n | T^{1f}(\mathbf{k}, \mathbf{q}, \mathbf{p}_n) | \lambda m_d \rangle = & -m \int \frac{d^3 \mathbf{p}_s}{(2\pi)^3} \frac{1}{p_{in}^2 - p_{out}^2 - i0} \\
& \times \sum_{m_{\tilde{p}} m_{\tilde{n}}} \left[\langle \mathbf{p}_{out}, m_p m_n | T_{np} | -\mathbf{p}_{in}, m_{\tilde{p}} m_{\tilde{n}} \rangle \langle m_{\tilde{p}} m_{\tilde{n}} | T^{1d}(\mathbf{k}, \mathbf{q}, \mathbf{p}_s) | \lambda m_d \rangle \right. \\
& \left. + \langle \mathbf{p}_{out}, m_p m_n | T_{np} | \mathbf{p}_{in}, m_{\tilde{p}} m_{\tilde{n}} \rangle \langle m_{\tilde{p}} m_{\tilde{n}} | T^{1e}(\mathbf{k}, \mathbf{q}, \mathbf{p}_s) | \lambda m_d \rangle \right]. \quad (3.10)
\end{aligned}$$

The amplitude (3.10) includes as subblocks the amplitudes (3.5) and (3.9) but with off-shell outgoing nucleons so that $p_{\pi N}^{*2}$ in Eq. (3.6) may be both positive and negative. One point which has to be emphasized is how to specify the energies in the loops. It is reasonable to suppose that the nucleon N'_S in the left loop is on its mass shell since such a choice precisely corresponds to that used when evaluating diagrams 1d and e. As to the right loop, a prescription for the nucleon energies used in the case of coherent π^0 photoproduction on the deuteron consisted in putting the recoil nucleon on its mass shell in the pion photoproduction vertex [10]. This prescription (which is referred to from here on as Case 1) was motivated by the location of the leading singularities of elementary amplitudes (the Δ pole singularity) and internal particle propagators. It was found in Ref. [10] that putting the recoil nucleon on its mass shell at the π - N vertex led to a one and a half times larger rescattering amplitude. We think, however, that the prescription above can hardly be considered as a hard-and-fast rule. Even a glance on Fig. 1f enables one to see that there are no reasons why such a choice of nucleon energies should be preferred. In fact, we have checked other realistic possibilities to specify the nucleon energies in the right loop. One of them was to suppose that each of the nucleons carried equal parts of the total energy of the final n - p pair, namely $(\varepsilon_n + \varepsilon_p)/2$ (Case 2). One more choice rejected in Ref. [10] was to put the recoil nucleon on its mass shell at the π - N vertex (Case 3).

Summations over polarizations of the particles in Eqs. (3.1)-(3.10) as well as the three-dimensional integrations in Eqs. (3.4), (3.5) and (3.9) and six-dimensional one in Eq. (3.10) have been carried out numerically making use of the methods described in Refs. [17,13]. Note, since Eq. (2.3) involves a three dimensional integration we were forced to carry out integrations with dimensions up to and including nine. Additional one-dimensional integrations were needed to solve the Lippmann-Schwinger equations for the N - N and π - N scattering amplitudes. The computing work was very hard but we were in a position with

reasonable computer resources to evaluate the integrals with a precision providing an accuracy of calculated cross sections better than 10%.

IV. RESULTS AND DISCUSSION

Based on the approach described in the previous section, we calculated the differential cross section (2.3) and total cross section of the reaction (1.1) in the energy region from the threshold ($E_{\gamma}^{thr} = 142.2$ MeV) to 160 MeV.

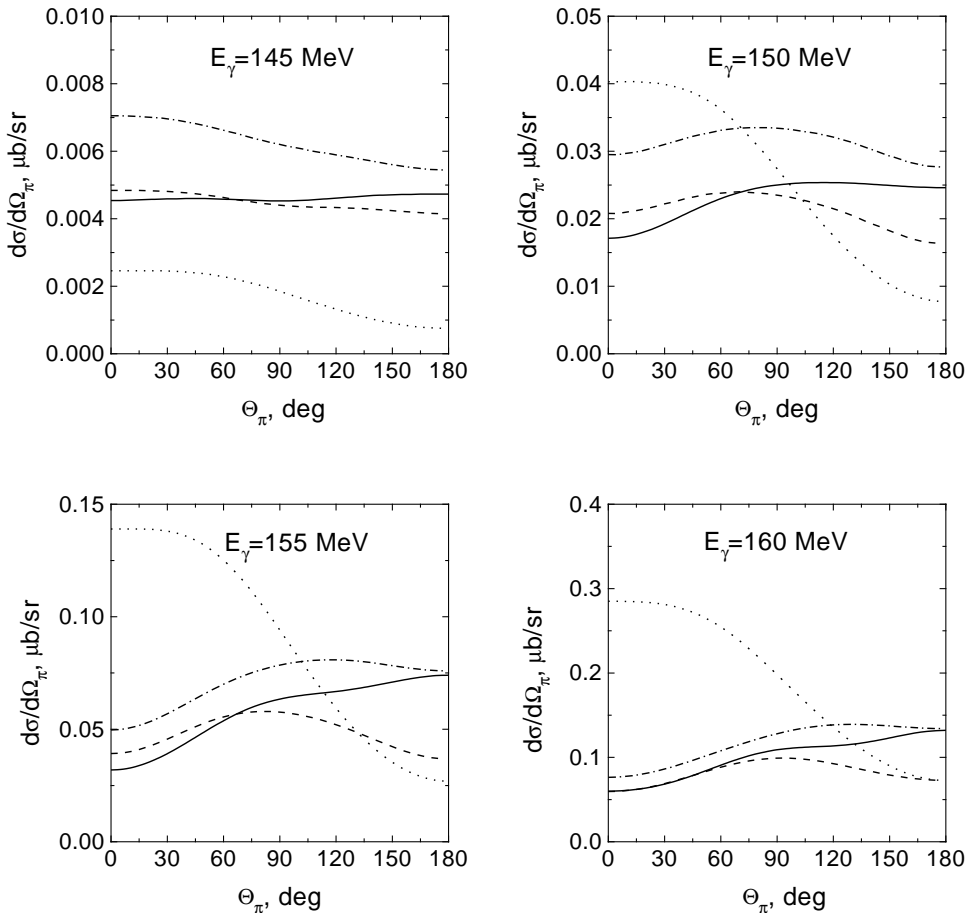


FIG. 2. Shown are contributions of different diagrams to the differential cross section (2.3) in the c.m. frame. Contribution of the pole diagrams 1a and b is given in dotted lines. Successive addition of the diagrams with n - p rescattering (1c), π - N rescattering (1d and e) and diagram 1f gives the dashed, dash-dotted and solid lines, respectively. The curves correspond to the ChPT set for the multipoles in Eq. (3.2) and Case 1 for nucleon energies in the right loop of diagram 1f.

In Fig. 2 we present our predictions for the differential cross section with the ChPT set for the multipoles in Eq. (3.2) and with the choice Case 1 for nucleon energies in the right loop of diagram 1f. One can see that the contributions of all the diagrams in Fig. 1 are of the same order so that none of the diagrams can be ignored in the calculation. The two pole diagrams give a forward-peaked angular distribution. This reflects the fact that the ChPT values of

the isospin averaged threshold electric dipole amplitude $E_{0+}^{(+)} = \frac{1}{2}[E_{0+}^{p\pi^0} + E_{0+}^{n\pi^0}] = 0.5$ and the amplitude $p_1^{(+)} = \frac{1}{2}[p_1^{p\pi^0} + p_1^{n\pi^0}] = 8.9$ are positive. Indeed, it is seen from Eq. (3.2) that the amplitudes $E_{0+}^{(+)}$ and $p_1^{(+)}$ are responsible for the forward-backward asymmetry in the differential cross section. An effect of $n-p$ final state interaction (diagram 1c) is strongly dependent on the photon energy. Just above threshold (e.g., at $E_\gamma=145$ MeV) it leads to increasing the differential cross sections over the full angular region and this increase is attributed to the strong attractive $n-p$ interaction in the singlet 1S_0 -state. At higher photon energies the repulsive triplet 3S_1 -interaction grows in importance. At $E \geq 150$ MeV the total effect of diagram 1c consists in a noticeable lowering of the cross sections except in the backward angle region.

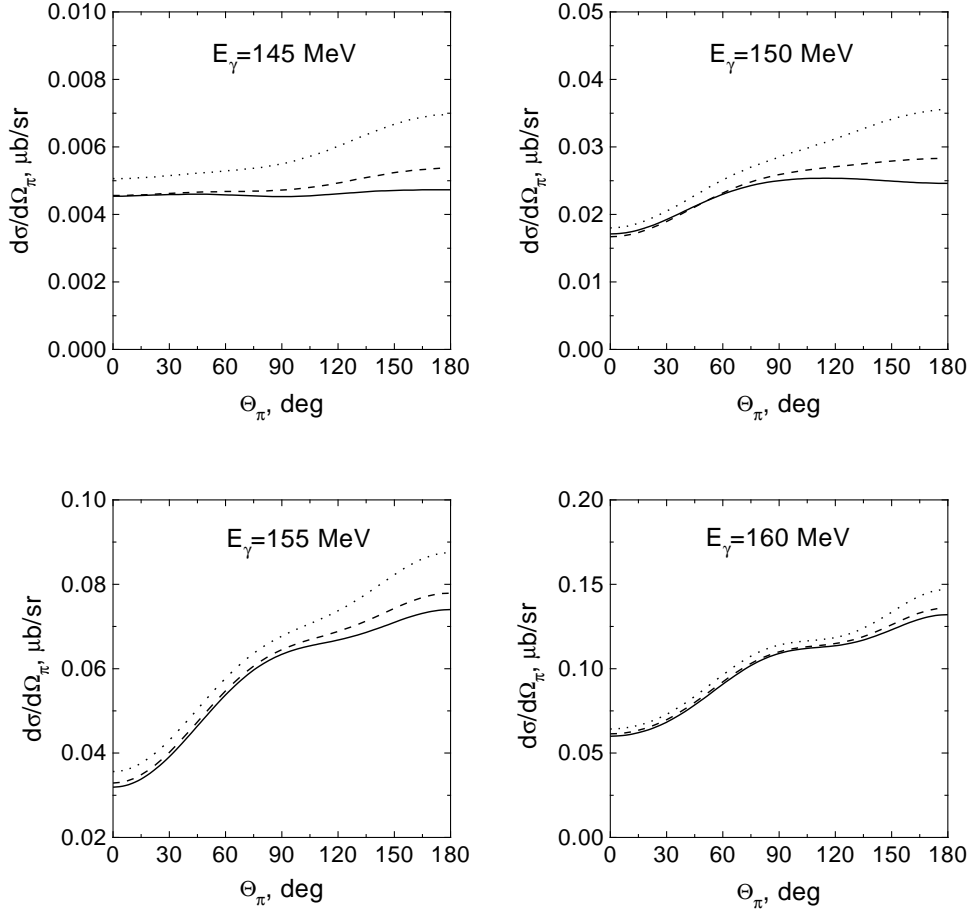


FIG. 3. Shown is the sensitivity of the differential cross section (2.3) in the c.m. frame to different prescriptions for nucleon energies in the right loop of diagram 1f: Case 1 (solid), Case 2 (dashed), Case 3 (dotted). The curves correspond to the ChPT set for the multipoles in Eq. (3.2).

As to diagrams 1d and e with $\pi-N$ rescattering in the final state, they increase the differential cross section at all angles. At $E \geq 155$ MeV these diagrams contribute mainly at backward angles. Finally, diagram 1f gives a noticeable reduction of the cross section at forward angles. It is seen in Fig. 2 that after inclusion of diagrams 1d to f the differential cross section becomes to be backward peaked at $E \geq 150$ MeV. This means that due to

π - N rescattering the amplitude $E_{0+}^{(+)}$ effectively acquires a negative contribution altering its sign. When making such a statement we suppose (and with some justice, see below) that although rescattering can also modify the $p_1^{(+)}$ amplitude the latter remains to be positive. This effect was first discovered in the framework of the ChPT [5] in the study of coherent π^0 photoproduction on the deuteron.

With the ChPT set for the multipoles in Eq. (3.2) we have calculated and presented in Fig. 3 the differential cross sections for various choices of nucleon energies in the right loop of diagram 1f. One can see that the results at $\Theta_\pi \leq 90^\circ$ are practically independent of the choice of the energies. This is not the case for backward angles. Case 1 leads to minimum cross sections and Case 3 to maximum ones. Results with Case 2 lie between. Simultaneously, with increasing photon energy the deviation is declining. It is worth mentioning that analogous observations were made in Ref. [7] in consideration of coherent π^0 photoproduction in the threshold region. It was found in that paper that various approximations for the nucleon kinetic energy at integrations over loops gave noticeable changes in the calculated differential cross sections especially near threshold and backward angles.

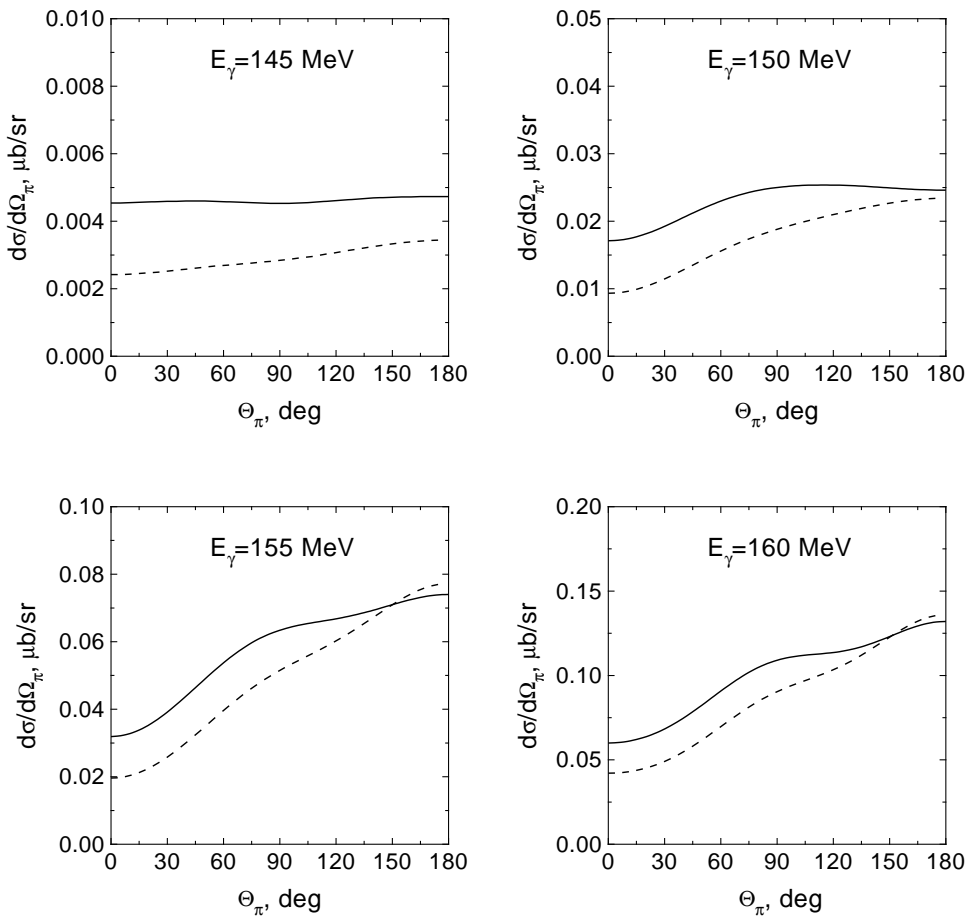


FIG. 4. Shown is the sensitivity of the differential cross section (2.3) in the c.m. frame to sets of the multipoles in Eq. (3.2): DR (dashed), ChPT (solid). The curves correspond to Case 1 for nucleon energies.

In Fig. 4 we compare our predictions for the angular distribution of the differential cross section with the ChPT and DR sets for the multipoles. It is seen that the ChPT and DR sets produce rather close cross sections at backward angles for $E_\gamma \geq 150$ MeV though there exist noticeable deviations at forward angles. In the energy region under consideration the DR sets produce only half of the ChPT cross sections at forward angles. This reflects the significant difference between the ChPT and DR predictions for the threshold electric dipole amplitude $E_{0+}^{n\pi^0}$ (see Sect. I) and the close consistency of the two for the $p_1^{(+)}$ amplitude.

The previous consideration shows that π - N rescattering (diagrams 1*d-f*) markedly changes the results calculated without this effect (diagrams 1*a-c*). It is instructive to study the question: what modification of the low energy parameters in the model without π - N rescattering is required in order to reproduce the predictions of the full model. We will be interested in the amplitudes $E_{0+}^{(+)}$ and $p_1^{(+)}$ only. Let us suppose that due to π - N rescattering these amplitudes acquire additional contributions $\Delta E_{0+}^{(+)}$ and $\Delta p_1^{(+)}$. Numerical estimates for them are obtained by switching off diagrams 1*d-f* and adjusting these parameters to reproduce the differential cross sections at $\Theta_\pi = 0^\circ$ and 180° for the full model. Our results are given in Table II. One comment should be made here. In a rigorous consideration the values $\Delta E_{0+}^{(+)}$ and $\Delta p_1^{(+)}$ must be independent of the parametrization for the low energy amplitudes in Eq. (3.2), i.e. the former should be the same for ChPT and DR amplitudes. Indeed, the difference between ChPT and DR manifests itself in the π^0 production amplitudes but the main contribution from π - N rescattering stems from charged pion exchanges. The slight difference for ChPT and DR results in Table II is because of a rather rough numerical method of extracting $\Delta E_{0+}^{(+)}$ and $\Delta p_1^{(+)}$. Nevertheless, we believe that such a method properly reproduces the tendency of variation of $E_{0+}^{(+)}$ and $p_1^{(+)}$ due to π - N rescattering. The dependence of $\Delta E_{0+}^{(+)}$ and $\Delta p_1^{(+)}$ on the choice of nucleon energies as seen in Table II is expected since the Cases 1 to 3 effectively lead to different pion propagators in Eq. (3.10).

Averaging over all values in Table II we obtain $\Delta E_{0+}^{(+)} \simeq -1.1$. One can see that $\Delta E_{0+}^{(+)}$ is negative in accordance with the ChPT result from Ref. [5] being, however, nearly two times smaller in the absolute value. The $p_1^{(+)}$ amplitude acquires a positive contribution an averaged value for which is 4.1 ± 0.6 . This result being put together with the free-nucleon value of about 9 gives $p_1 = 13.1 \pm 0.6$ and reasonably reproduces an experimental result of Ref. [6], $p_1^{exp} = 12.88 \pm 0.28$. In other words, our estimates confirm an assumption from that paper that a mechanism responsible for renormalizing the p_1 amplitude is the two-body process corresponding to π - N rescattering.

TABLE II. Effective modifications of the threshold $E_{0+}^{(+)}$ and $p_1^{(+)}$ amplitudes due to π - N rescattering. Units are conventional.

	Case 1		Case 2		Case 3	
	$\Delta E_{0+}^{(+)}$	$\Delta p_1^{(+)}$	$\Delta E_{0+}^{(+)}$	$\Delta p_1^{(+)}$	$\Delta E_{0+}^{(+)}$	$\Delta p_1^{(+)}$
ChPT	-1.2	+3.7	-1.1	+4.2	-1.2	+4.7
DR	-1.0	+3.5	-1.1	+3.8	-1.1	+4.5

To make it much easier using our results in practice, we have parametrized the differential

cross sections at four photon energies 145, 150, 155, and 160 MeV with the help of the following formula

$$\frac{d\sigma}{d\Omega_\pi} = A_1 + A_2 \cos \Theta_\pi, \quad (4.1)$$

with parameters given in Table III. The values for A_1 and A_2 have been obtained by a fit to the average of the minimum and the maximum cross sections (see above) and the errors in A_1 account for variations of the cross sections both due to various choices of sets for multipoles and nucleon energies in the right loop of diagram 1f. The corresponding cross sections at arbitrary energies up to 160 MeV can be obtained by making use of a suitable interpolation procedure. We think that such a simple parametrization provides reasonable accuracy to be used in estimates of inelastic channel contributions to coherent π^0 production.

TABLE III. Coefficients A_1 and A_2 in Eq. (4.1) at four selected photon energies. Units are $\mu\text{b}/\text{sr}$.

	145 MeV	150 MeV	155 MeV	160 MeV
A_1	0.0043 ± 0.0014	0.023 ± 0.005	0.057 ± 0.007	0.095 ± 0.012
A_2	-0.0007	-0.007	-0.026	-0.041

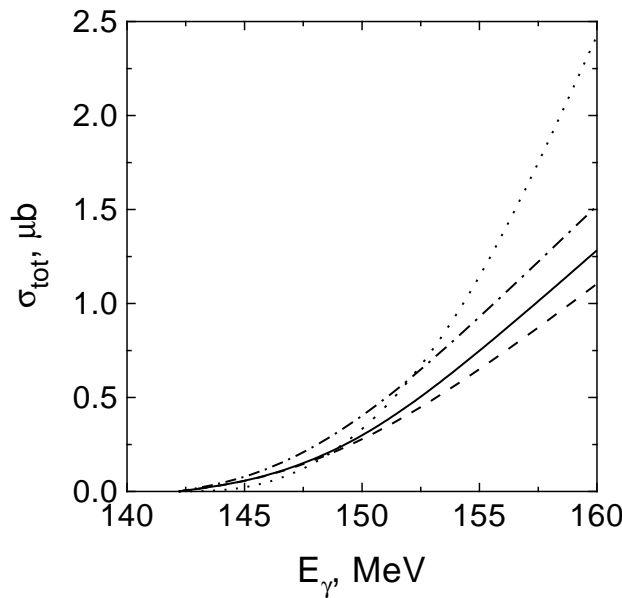


FIG. 5. Total cross section of the reaction $^2H(\gamma, \pi^0)np$ in the threshold region as a function of photon lab energy. Meaning of curves as in Fig. 2.

Performing in Eq. (2.3) an integration over the pion solid angle Ω_π we can calculate the total cross section σ_{tot} of the reaction (1.1) (note that $\sigma_{\text{tot}} = 4\pi A_1$ where σ_{tot} is in units of μb). In Fig. 5 we show contributions of different diagrams to σ_{tot} with the ChPT set for

the multipoles in Eq. (3.2). The two pole diagrams produce a total cross section which is rapidly increasing with photon energy. After inclusion of the $n-p$ final state interaction the energy distribution of σ_{tot} becomes to be more flat. Just above threshold this interaction in the 1S_0 -wave leads to an increase of σ_{tot} but at $E_\gamma \geq 155$ MeV the cross section diminishes by a factor of about 2. Diagrams 1d and e with $\pi-N$ rescattering give noticeable positive contribution to the total cross section. Of all the diagrams 1f is the least important one, decreasing σ_{tot} by about 10%.

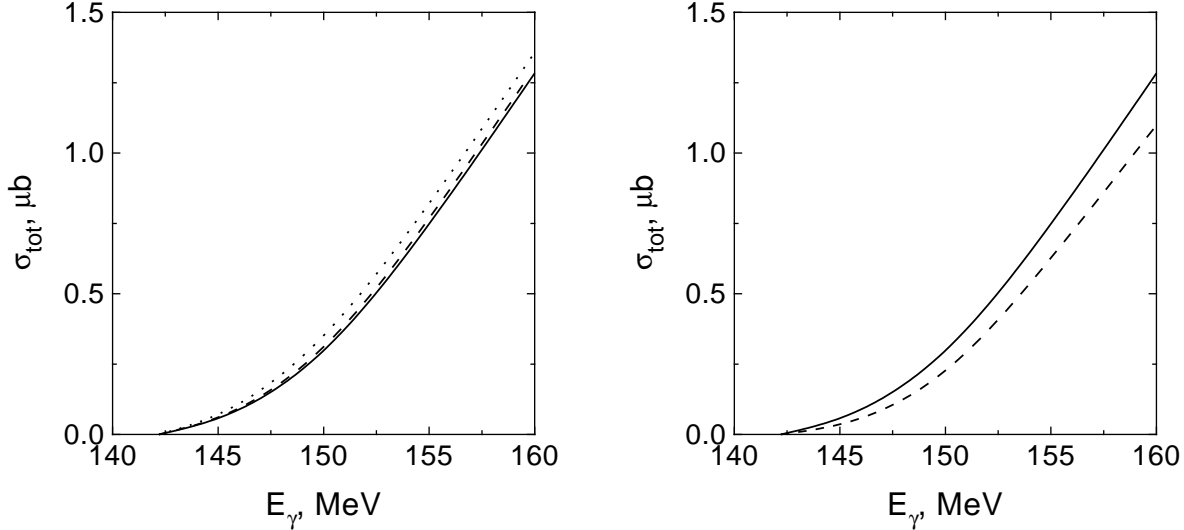


FIG. 6. Left panel: shown is the sensitivity of the total cross section to different prescriptions for nucleon energies in the right loop of diagram 1f. Meaning of curves as in Fig. 3. Right panel: sensitivity of the total cross section to sets of the multipoles in Eq. (3.2). Meaning of curves as in Fig. 4.

The total cross sections for various choices of nucleon energies in the right loop of diagram 1f are presented in the left panel of Fig. 6. It is seen that they are practically independent of a prescription for the energy. This reflects the smallness of the diagram 1f contribution to the total cross section. Our predictions for σ_{tot} with the ChPT and DR sets of the multipoles are also shown in Fig. 6. There is a deviation of about 15% in the full energy region.

In Fig. 7 we compare our results with the ones of the model [6] for the differential and total cross sections. One can see that the predictions of the two calculations are quite consistent. There is some disagreement at $E_\gamma \geq 155$ MeV and forward angles for the differential cross section. It should be emphasized, however, that this disagreement cannot make any noticeable changes in the cross sections of coherent π^0 photoproduction measured in Ref. [6] because of smallness of the inelastic channel cross sections in comparison with the coherent channel ones. At the same time, at backward angles the inelastic channel is growing in importance but there the deviation is not very significant. One can see that the maximum deviation between the present calculation and the one of Ref. [6] does not exceed 20% at 160 MeV and backward angles, being even smaller when the energy is decreasing. (Note here that the authors of that paper ascribed to their calculated cross sections of the

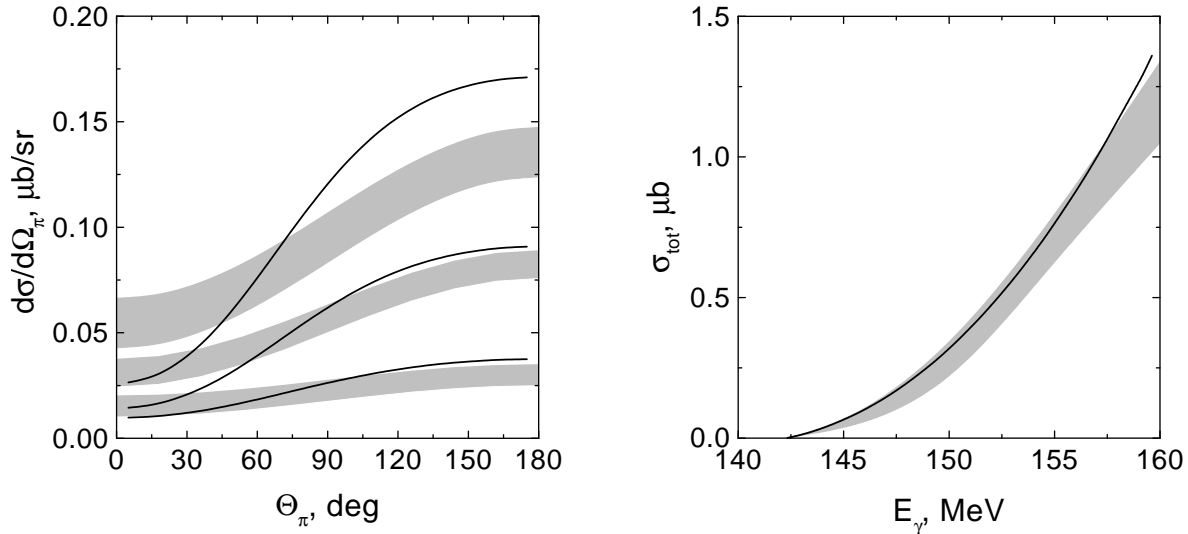


FIG. 7. Left panel: shown are errors bars (filled areas) in the differential cross sections stemming from various prescriptions for nucleon energies and different sets of multipoles at 150, 155, and 160 MeV (from bottom to top) calculated with Eq. (4.1) and coefficients A_1 and A_2 from Table III. Curves are results of Ref. [6]. Right panel: the same as for the left panel but for the total cross section.

inelastic channel uncertainties of about $\pm 25\%$ which were taken into account in their data analysis). In the case of the total cross section we observe good agreement with Ref. [6]. An analysis performed by Bergstrom [18] has shown that the p_1 amplitude is insensitive to the variation in the inelastic cross section from the present work and that from Ref. [6]. Likewise, the extrapolation of the E_d amplitude to threshold changes very little, remaining within the error in Eq. (12) of Ref. [6].

In summary, we have performed an investigation of the reaction ${}^2H(\gamma, \pi^0)np$ in the threshold region and found a good agreement with the only previous calculation [6] for the total cross section. A reasonable agreement also exists for the differential cross sections. Our predictions coincide within of 20%. If one takes into account that the authors of that work ascribed to their results an uncertainty of about $\pm 25\%$ we conclude that the present calculation cannot lead to any changes in the total and differential cross section of coherent π^0 photoproduction on the deuteron measured in Ref. [6]. This means that the deviation of about 20% from theoretical predictions found in that paper for the E_d threshold amplitude still remains to be resolved. Our calculations have shown that the difference of about $4 \cdot 10^{-3}/\mu_{\pi^+}^3$ between the free-nucleon value for the p_1 threshold amplitude and the experimental value can be attributed to two-body effects due to π - N rescattering.

ACKNOWLEDGMENTS

We would like to thank J.C. Bergstrom for supplying us with results of his numerical calculations and for fruitful discussions. We are pleased to acknowledge helpful comments by A.I. L'vov. One of the authors (M.L.) is indebted to M.V. Galynsky for the use of

his computer. This work was supported by Advance Research Foundation of Belarus and Deutsche Forschungsgemeinschaft under contract 436 RUS 113/510.

REFERENCES

- [1] V. Bernard, N. Kaiser and U.-G. Meißner, Phys. Lett. B 378 (1996) 337.
- [2] O. Hanstein, D. Drechsel and L. Tiator, Phys. Lett. B 399 (1997) 13.
- [3] J.C. Bergstrom, J.M. Vogt, R. Igarashi, K.J. Keeter, E.L. Hallin, G.A. Retzlaff, D.M. Skopik and E.C. Booth, Phys. Rev. C 53 (1996) R1052.
- [4] M. Fuchs, J. Ahrens, G. Anton, R. Averbeck, R. Beck, A.M. Bernstein, A.R. Gabler, F. Haerter, P.D. Harty, S. Hlavac, B. Krusche, I.J.D. McGregor, V. Metag, R. Novotny, R.O. Owens, J. Peise, M. Roebig-Landau, A. Schubert, R.S. Simon, H. Stroehrer and V. Tries, Phys. Lett. B 368 (1996) 20.
- [5] S.R. Beane, V. Bernard, T.-S.H. Lee, U.-G. Meißner and U. van. Kolck, Nucl. Phys. A 618 (1997) 381.
- [6] J.C. Bergstrom, R. Igarashi, J.M. Vogt, N. Kolb, R.E. Pywell, D.M. Skopik and E. Korkmaz, Phys. Rev. C 57 (1998) 3203.
- [7] M. Benmerrouche and E. Tomusiak, Phys. Rev. C 58 (1998) 1777.
- [8] M.I. Levchuk, V.A. Petrun'kin and M. Schumacher, Z. Phys. A 355 (1996) 317.
- [9] J.H. Koch and R.M. Woloshyn, Phys. Rev. C 16 (1977) 1968.
- [10] P. Bosted and J.M. Laget, Nucl. Phys. A 296 (1978) 413.
- [11] R. Machleidt, K. Holinde and Ch. Elster, Phys. Rep. 149 (1987) 1.
- [12] R. Machleidt, Adv. Nucl. Phys. 19 (1989) 189.
- [13] M.I. Levchuk, Few-Body Systems 19 (1995) 77.
- [14] I. Blomqvist and J.M. Laget, Nucl. Phys. A 280 (1977) 405.
- [15] J.M. Laget, Phys. Rep. 69 (1981) 1.
- [16] S. Nozawa, B. Blankleider and T.-S.H. Lee, Nucl. Phys. A 513 (1990) 459.
- [17] M.I. Levchuk, A.I. L'vov and V.A. Petrun'kin, Few-Body Systems 16 (1994) 101.
- [18] J.C. Bergstrom, private communication.